Patched regulates Smoothened trafficking using lipoprotein-derived lipids

Helena Khaliullina, Daniela Panáková, Christina Eugster, Falko Riedel, Maria Carvalho and Suzanne Eaton*

Hedgehog (Hh) is a lipoprotein-borne ligand that regulates both patterning and proliferation in a wide variety of vertebrate and invertebrate tissues. When Hh is absent, its receptor Patched (Ptc) represses Smoothened (Smo) signaling by an unknown catalytic mechanism that correlates with reduced Smo levels on the basolateral membrane. Ptc contains a sterol-sensing domain and is similar to the Niemann-Pick type C-1 protein, suggesting that Ptc might regulate lipid trafficking to repress Smo. However, no endogenous lipid regulators of Smo have yet been identified, nor has it ever been shown that Ptc actually controls lipid trafficking. Here, we show that *Drosophila* Ptc recruits internalized lipoproteins to Ptc-positive endosomes and that its sterol-sensing domain regulates trafficking of both lipids and Smo from this compartment. Ptc utilizes lipids derived from lipoproteins to destabilize Smo on the basolateral membrane. We propose that Ptc normally regulates Smo degradation by changing the lipid composition of endosomes through which Smo passes, and that the presence of Hh on lipoproteins inhibits utilization of their lipids by Ptc.

KEY WORDS: Hedgehog, Patched, Smoothened, Lipid, Lipoprotein, *Drosophila*

INTRODUCTION

The Hedgehog (Hh) signaling pathway is a highly conserved regulator of growth and differentiation that is essential for both vertebrate and invertebrate development (Ingham and Placzek, 2006; McMahon et al., 2003). Its misregulation in adult life leads to the formation of a variety of different tumors (Dellovade et al., 2006; Pasca di Magliano and Hebrok, 2003; Ruiz i Altaba et al., 2002). Hh signals by regulating the level and activity of the transcription factor Cubitus interruptus (Ci). It does so by binding to the transmembrane receptor Patched (Ptc) and preventing Ptc from repressing signaling by the seven-transmembrane domain protein Smoothened (Smo). Smo signaling then prevents processing of the full-length Ci_{155} to a repressor form (Ci_{75}), and promotes nuclear translocation and activation of Ci_{155}, apparently by separable mechanisms (Aza-Blanc and Kornberg, 1999; Kalderon, 2005; Lefers et al., 2001; Lum and Beachy, 2004; Nybakken and Perrimon, 2002; Smelkinson et al., 2007).

In the absence of Hh, Ptc catalytically represses Smo activity (Taipale et al., 2002) by a mechanism that correlates with changes in Smo subcellular localization. In *Drosophila*, Ptc decreases Smo stability and inhibits its accumulation on the basolateral membrane (Denef et al., 2000). In vertebrate cells, Ptc prevents Smo accumulation in the primary cilium where downstream components of the signal transduction pathway are located (Corbit et al., 2005; Haycraft et al., 2005; Huangfu and Anderson, 2005; Huangfu and Anderson, 2006; Rohatgi et al., 2007). Although localization of Smo to primary cilia is required for Smo-dependent target gene activation, it is not sufficient – deletion of the Smo N terminus or treatment with the Smo antagonist cyclopamine both cause Smo to traffic into cilia but inhibit its signaling activity. Other Smo antagonists appear to act by blocking ciliary localization, suggesting

that Smo activity might be regulated at multiple steps by different ligands (Aanstad et al., 2009; Rohatgi et al., 2009; Wang et al., 2009).

The mechanisms by which Ptc exerts these effects are not completely understood. Ptc is one of a family of sterol-sensing domain (SSD) proteins that includes SCAP [sterol regulatory element-binding protein (SREBP) cleavage-activating protein] and NPC1 (the protein encoded by the Niemann-Pick type C-1 disease gene), all of which are structurally related to the larger RND (resistance nodulation division) family of proton-driven transmembrane transporters (Tseng et al., 1999). The nearest relative of the Ptc proteins, NPC1, promotes the mobilization of glycosphingolipids and low-density lipoprotein (LDL)-derived cholesterol from late endosomes to other cellular membranes in both *Drosophila* and vertebrates (Ikonen and Holtta-Vuori, 2004; Mukherjee and Maxfield, 2004). A functional Ptc SSD is essential for Smo repression (Martin et al., 2001), raising the possibility that lipid trafficking may be involved in this process. Smo repression also requires regions in the Ptc C-terminal tail, which promote Ptc internalization and turnover (Lu et al., 2006). Vertebrate Smo signaling can be artificially repressed or activated by the binding of a variety of small lipophilic compounds (Chen et al., 2002a; Chen et al., 2002b; Frank-Kamenetsky et al., 2002), supporting the possibility that related lipids may regulate Smo activity in vivo. However, whether these small molecules mimic the activity of endogenous cellular lipids is not clear. Vertebrate Smo activity can be increased by oxysterols, however these do not appear to bind to Smo directly (Corcoran and Scott, 2006; Dwyer et al., 2007). Furthermore, whether Ptc actually regulates lipid trafficking remains to be established.

Hh associates with the *Drosophila* lipoprotein particle Lipophorin (Lpp) (Panáková et al., 2005) and these particles are necessary for normal Hh signaling (Callejo et al., 2008; Panáková et al., 2005). Here, we show that specific lipids contained within Lpp are required to decrease Smo levels and Smo-dependent Ci_{155} stabilization in the absence of Hh. Ptc recruits a small fraction of internalized Lpp to Ptc-positive endosomes and regulates both lipid trafficking and Smo trafficking from this compartment.

Max Planck Institute of Molecular Cell Biology and Genetics, Pfotenhauerstrasse-108, 01307 Dresden, Germany.

*Author for correspondence (eaton@mpi-cbg.de)

MATERIALS AND METHODS

Drosophila stocks

Transgenes: *UAS<HcRed>dsLpp* (Panáková et al., 2005), *dpplacZ^BS3.0* (Blackman et al., 1991), *UAS-Ptc* (Martin et al., 2001), *UAS-Ptc^S2 GFP* (Torroja et al., 2004), *UASPtc^SSD* (Martin et al., 2001), *UAS-Ptc^Dloop2* (Briscoe et al., 2001), *UAS-Ptc^I130x* (Johnson et al., 2000), *tubP-CFPRab5* (Marois et al., 2006), *UAS<HcRed>Rab7TN* (Marois et al., 2006), *ap-GAL4* (Rincon-Limas et al., 1999), *Adh-GAL4*, *Tub-GAL4* and *tubP-GAL80^ts* (Bloomington). Mutants: *disp^S037707* (Burke et al., 1999), *boca^1* (Culi and Mann, 2003), *smo^3* (Chen and Struhl, 1998), *hh^ts2* (Strigini and Cohen, 1997), *ptc^IIw* (also known as *Ptc^16*) (Strutt et al., 2001) and *ptc^S2* (Martin et al., 2001).

Transgenes

Transgenic flies expressing double-stranded RNA (dsRNA) against *LRP1* or *Megalin* RNAi were made using pFRiPE (Marois et al., 2006). We used a repeat unit corresponding to nucleotides 10671-11112 of CG33087-RC for *LRP1* and nucleotides 11821-12342 of CG12139-RB for *Megalin*. *UAS<HcRed>Rab9S21N* was made by insertion of rab9S21N (Riederer et al., 1994) into pFRIPE (Marois et al., 2006).

Induction of RNAi

LppRNAi was induced as described (Panáková et al., 2005) using Adh-GAL4 to drive fat body expression. Larvae containing *Arrow*, *Megalin* and *LRP1* RNAi constructs under the control of apGAL4 were heat shocked at 37°C for 90 minutes to excise the intervening *HcRed* cassette, reared at 29°C and dissected after 48 hours.

Clonal analysis

boca^1 clones were generated as described (Culi and Mann, 2003). *ptc^S2* and *ptc^IIw* clones were generated as described (Martin et al., 2001) For *smo^3* null clones, *hsp70-flp; smo^3, FRT40A/Ubi-GFPnls, FRT40A; +/TubGAL4* and *hsp70-flp; smo^3, FRT40A/Ubi-GFPnls, FRT40A; UAS<HcRed>dsLpp/TubGAL4* larvae were heat shocked at 37°C for 90 minutes, reared at 25°C and dissected after 108 hours.

Induction of Ptc transgenes

Ap-GAL4, *tubP-GAL80^ts*/UAS-Ptc animals were reared at 18°C and third instar larvae were transferred to 29°C for 15-18 hours. Ap-GAL4, *tubP-GAL80^ts*/UAS-Ptc; *hh^ts2/hh^ts2* larvae were treated similarly.

Immunohistochemistry

Imaginal discs were fixed and stained as described previously (Marois et al., 2006). Antibodies were diluted as follows: anti-Ci 2A1 1:10 (Wang and Holmgren, 1999), anti-β-gal 1:100 (Promega Z378A), anti-Ptc 1:100 (DSHB, University of Iowa, Department of Biological Sciences, Iowa City, IA 52242, USA), anti-Smo 1:50 (Lum et al., 2003), anti-Megalin 1:1000, anti-LRP1 1:1000, anti-Hh 1:500 (Panakova et al., 2005) and anti-Lpp guinea pig 1:1000 (Eugster et al., 2007).

Antisera

For anti-LRP1 we immunized rabbits with a glutathione-S transferase (GST) fusion to amino acids 4607-4699 of CG33087-PC (Eurogentec, Seraing, Belgium). For anti-Megalin, a peptide corresponding to amino acids 4533-4547 of CG12139-PB was conjugated to keyhole limpet hemocyanin (KLH) and used to immunize guinea pigs (Antibodies Inc., Davis, CA, USA). Rabbit anti-Ptc was generated against the second extracellular loop and used at 1:300.

Leptomycin B treatment

Imaginal discs were dissected in Grace's insect medium and incubated for 90 minutes at 28°C with 20 nM of leptomycin B (Sigma) before fixation.

Western blotting

Membranes were incubated with anti-Ci 1C2 1:5 (Wang and Holmgren, 1999) and anti-actin 1:1000 (Sigma); followed by HRP-conjugated anti-rat IgM 1:2000 and anti-rabbit IgG 1:5000 (Dianova), respectively.

Image analysis

For confocal images, the position below the apical surface corresponds to 0.7-2.8 μm for the apical region, 1.4-2.1 μm for the sub-apical region and 2.1-4.8 μm for the basolateral (or middle) region.

All quantified immunostaining was performed on discs that were dissected, fixed, stained and imaged in parallel using the same microscope settings. To quantify Ci and Smo staining intensities, three apical sections, 0.7 μm apart, were projected using maximal intensity in ImageJ. For each image, two rectangles of 100 pixels parallel to the anteroposterior (AP) axis by 351 pixels parallel to the dorsoventral (DV) axis were selected and centered at the AP boundary in ventral and dorsal compartments. Average pixel intensity was determined as a function of distance from the AP boundary using PlotProfile and plotted using Microsoft Excel. All AP boundaries were determined according to anti-Ci or anti-Ptc co-immunostaining.

To estimate the significance of changes in staining intensities in discs of different genotypes, we measured Smo or Ci staining intensity at the same distance from the AP boundary in each disc and calculated *P* values using Excel. To quantify the colocalization percentage, we used the colocalization plugin of the Fiji image processing software.

Statistical significance was determined according to Costes et al. (Costes et al., 2004), where *P* value$_{Costes}$=1 − the fraction of randomized images giving a Pearson correlation coefficient greater than the original image.

Isolation of Lpp particles

Lpp particles were isolated from third instar larvae by first breaking them with a loose pestle and then pelleting tissues and larval carcasses at 1000 *g* for 10 minutes. Supernatants were spun at 33,600 rpm (142,000 *g*) for 3 hours in a SW40Ti rotor to remove debris and KBr was then added to a concentration of 0.33 g/ml and spun at 39,000 rpm (192,000 *g*) for 64 hours in a SW40Ti rotor. The top fraction was removed and desalted on a Sephadex column.

Pulse chase with labeled Lpp particles

Desalted Lpp particles (see above) were labeled with an amine-reactive Alexa 546 probe (Molecular Probes), as described (Panáková et al., 2005). Ap-GAL4, *tubP-GAL80^ts*/UAS-Ptc larvae, reared at 29°C for 18 hours, were dissected in Grace's medium and incubated with labeled Lpp particles (at a protein concentration of 0.5 mg/ml in Grace's medium) for 10 minutes at 22°C. Ten minutes is the minimum time required to see uptake of labeled dextran by imaginal disc cells (Marois et al., 2006). The discs were then either washed immediately in PBS at 4°C and fixed (4% PFA for 20 minutes at room temperature), or washed and incubated for varying times in Grace's medium at 22°C before fixation.

Rescue with lipids

Lipids were extracted from purified Lpp particles by a two-step Bligh and Dyer method (Bligh and Dyer, 1959). Total lipid concentration was measured according to Marsh and Weinstein (Marsh and Weinstein, 1966). Liposomes were prepared from dried lipids by sonication for 30 minutes into Grace's medium to produce a final total lipid concentration of 500 μg/ml. Assuming that hemolymph represents approximately half of the larval volume, this concentration should be similar to that of the lipids contributed by the Lpp fraction of the hemolymph. Wing imaginal discs from *hsp70-flp/+; Adh-GAL4/+; UAS<HcRed>dsLpp/+* larvae were incubated in Grace's medium or in Grace's medium with liposomes for 2 hours at 22°C. Discs were fixed and stained as described previously (Marois et al., 2006).
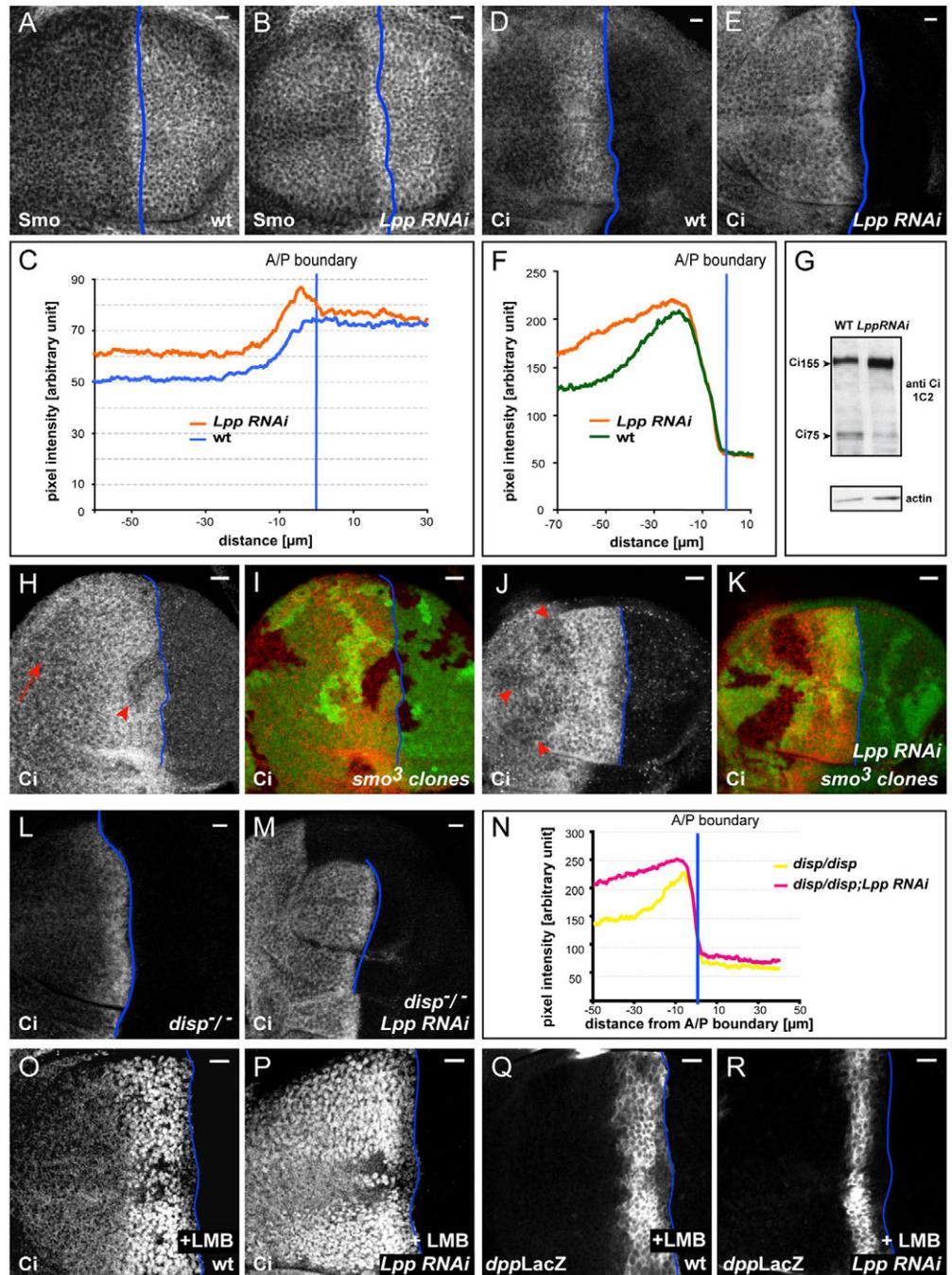
RESULTS

Lpp is required to reduce Smo accumulation on the basolateral membrane

Lpp particles are made in the fat body and travel through the hemolymph to imaginal discs where they bind to Hh and are required for long-range Hh trafficking and target gene activation (Panáková et al., 2005). As we investigated how loss of Lpp affected individual components of the Hh signal transduction machinery, we made the unexpected discovery that these particles also function to repress a subset of Hh signaling events when Hh is absent.

Ptc-mediated Smo repression correlates with the post-transcriptional destabilization of Smo protein and reduces Smo levels at the basolateral membrane (Denef et al., 2000). To investigate the consequences of reduced Lpp levels on Smo trafficking, we compared the accumulation of Smo protein in wild-

Fig. 1. Lpp RNAi increases basolateral Smo accumulation and Smo-dependent Ci stabilization independently of Hh. (**A**,**B**) Smo staining in the basolateral region of a wild-type (A) and a LppRNAi (B) wing disc. Smo levels are elevated in the anterior compartment of the LppRNAi disc. (**C**) Quantification of Smo staining from 19 wild-type and 10 LppRNAi discs. Smo staining is elevated by LppRNAi in the anterior compartment ($P<0.0006$ for anterior, $P<0.4908$ for posterior). (**D**,**E**) Wing discs from a wild-type and a LppRNAi animal stained for Ci_{155}. The range of Ci_{155} stabilization is extended in the LppRNAi wing disc. (**F**) Quantification of Ci_{155} staining intensity in at least 14 wild-type and 14 LppRNAi discs ($P<0.0059$). (**G**) Western blot of disc extracts from wild-type and LppRNAi animals probed with 1C2, detecting both Ci_{75} and Ci_{155}, and for actin. The average band intensities for Ci_{155} and Ci_{75} were quantified and compared with those of actin: $(Ci_{155}/actin)_{LppRNAi}=1.7$, $(Ci_{155}/actin)_{wild\ type}=1.3$, $(Ci_{75}/actin)_{LppRNAi}=0.4$, $(Ci_{75}/actin)_{wild\ type}=1.0$. LppRNAi increases Ci_{155} levels at the expense of Ci_{75}. (**H**,**I**) Wild-type wing disc harboring *smo* clones [lack of green fluorescent protein (GFP) in I], stained for Ci_{155} (H and I, red). The red arrowhead indicates a loss of Ci_{155} in a *smo* clone near the AP boundary. The red arrow indicates unchanged Ci_{155} in a *smo* clone far from the AP boundary. (**J**,**K**) Wing disc from a LppRNAi animal harboring *smo* clones, stained for Ci_{155} (J and K, red). Lack of GFP (K, green) indicates a loss of *smo*. Red arrowheads indicate reduced Ci_{155} levels in *smo* clones, even those far from the AP boundary. (**L**) A *disp*$^{-/-}$ wing disc

stained for Ci_{155}. The range of Ci_{155} stabilization is reduced. (**M**) A *disp*$^{-/-}$;LppRNAi wing disc stained for Ci_{155}. Ci_{155} accumulates throughout the anterior compartment. (**N**) Quantification of Ci_{155} staining in *disp*$^{-/-}$ wing discs with and without induction of LppRNAi. At least two discs were quantified for each condition. (**O**,**Q**) A *dpplacZ* wing disc treated for 1.5 hours with leptomycin B and then stained for Ci_{155} (O) and *lacZ* (Q). Ci_{155} accumulates in nuclei where it activates *decapentaplegic* (*dpp*) transcription over its normal range. (**P**,**R**) A *dpplacZ* wing disc, 5 days after the induction of LppRNAi, treated for 1.5 hours with leptomycin B and then stained for Ci_{155} (P) and *lacZ* (R). Ectopically stabilized Ci_{155} translocates to the nucleus throughout the anterior compartment, but the transcription of *dpplacZ* is narrowed. Occasionally, DpplacZ is slightly elevated throughout the anterior compartment when LppRNAi discs are treated with leptomycin B (see Fig. S2E,F in the supplementary material), but this is never observed in the absence of leptomycin B. AP boundaries are indicated by blue lines. Scale bars: 10 μm.

type wing discs with LppRNAi wing discs. Although *smo* is transcribed uniformly throughout the wing pouch, Ptc activity reduces Smo protein levels on the basolateral membrane of most anterior compartment cells in wild-type discs. Smo accumulates to a high level only in the posterior compartment, which does not

express Ptc, and in the anterior compartment near the AP boundary, where Hh inhibits Ptc activity (Fig. 1A,C) (Denef et al., 2000). Strikingly, LppRNAi strongly increases Smo protein levels on the basolateral membrane throughout the anterior compartment, but has little effect on Smo accumulation in posterior cells (Fig. 1B,C). This

is surprising because LppRNAi does not expand the range of activation of any Hh target gene. Indeed, Lpp knockdown narrows the range of Hh target gene activation (Fig. 1Q,R) (Callejo et al., 2008; Panáková et al., 2005). Despite the reduced range of target gene activation in LppRNAi discs, Smo actually accumulates on the basolateral membrane as it would if Ptc activity were reduced. This disconnection between Smo trafficking and target gene activation resembles the situation in cyclopamine-treated vertebrate cells, where inactive Smo accumulates in primary cilia ligands (Aanstad et al., 2009; Rohatgi et al., 2009; Wang et al., 2009).

Lpp knockdown increases Smo-dependent Ci$_{155}$ stabilization

To investigate why target genes were not activated by the accumulation of Smo in LppRNAi discs, we first asked whether Smo was able to induce stabilization of the full-length form of the transcriptional activator Ci$_{155}$. In wild-type discs, antibodies that recognize only full-length Ci$_{155}$ show that it is stabilized by Smo signaling over a distance of 40 μm (12-15 cell diameters) from the posterior Hh-producing cells (Fig. 1D,F) (Aza-Blanc et al., 1997). When Lpp levels are reduced by RNAi, full-length Ci$_{155}$ staining is elevated, both near the AP boundary where Hh is present, and throughout the entire anterior compartment (Fig. 1E,F). Thus, increasing levels of basolateral Smo is enough to stabilize Ci$_{155}$.

To confirm that Lpp knockdown caused Ci$_{155}$ accumulation by preventing processing to Ci$_{75}$, we performed western blotting using imaginal disc extracts and an antibody that detects both Ci$_{155}$ and Ci$_{75}$. LppRNAi increases the ratio of full-length Ci$_{155}$ to that of the repressor Ci$_{75}$ (Fig. 1G). Thus, Lpp knockdown not only causes Smo to accumulate, but increases its capacity to stabilize Ci$_{155}$. These effects are not an indirect consequence of a failure to mobilize dietary lipids, because transfer to lipid-depleted medium does not mimic the effects of LppRNAi (see Fig. S1A-G in the supplementary material). Instead, the effects are caused by the direct action of Lpp particles on imaginal discs; addition of purified Lpp particles to explanted discs reversed both Smo accumulation and Ci$_{155}$ stabilization (see Fig. S1H-O in the supplementary material).

To confirm that ectopic Ci$_{155}$ accumulation required Smo, we induced *smo* mutant clones in LppRNAi animals and stained their wing imaginal discs with an antibody to Ci$_{155}$. In wild-type discs, Ci$_{155}$ is destabilized by loss of Smo only in cells near the AP boundary where Smo signaling is activated by Hh (Fig. 1H arrowhead, I). Low levels of Ci$_{155}$ are detected further away from the AP boundary, but do not require Smo since they are not reduced in *smo* clones (Fig. 1H arrow, I). In LppRNAi animals, the ectopically stabilized Ci$_{155}$ that is far from the AP boundary is also reduced by *smo* loss of function; Ci$_{155}$ is reduced in *smo* clones even when they lie on the anterior edge of the disc where Hh is not detectable (Fig. 1J arrowheads, K). Thus, elevated Ci$_{155}$ levels in LppRNAi discs depend on Smo.

To confirm that the increased level of Ci$_{155}$ in LppRNAi animals was Hh-independent, we asked whether LppRNAi could still stabilize Ci$_{155}$ in a *dispatched* (*disp*) mutant background. Disp is required for Hh secretion. Zygotic mutants survive to the third larval instar, but fail to secrete Hh as maternal Disp is depleted (see Fig. S2A in the supplementary material) (Burke et al., 1999). As a result, the range of Ci$_{155}$ stabilization is strongly reduced in these discs (Fig. 1L). When LppRNAi is induced in a *disp* mutant background, no Hh is observed in receiving tissue (see Fig. S2B in the supplementary material). Nevertheless, Ci$_{155}$ is stabilized just as efficiently as when Disp is present and Hh is secreted (Fig. 1M,N). Thus, loss of Lpp stabilizes Ci$_{155}$ independently of Hh.

Smo-mediated Ci stabilization and nuclear translocation are insufficient for target gene activation

In addition to stabilizing Ci$_{155}$, Smo signaling promotes the release of Ci$_{155}$ from microtubule-associated multiprotein complexes, allowing its nuclear translocation. To test whether Ci$_{155}$ that is ectopically stabilized by Lpp knockdown was able to enter the nucleus, we treated discs with leptomycin B to block nuclear export and stained them for Ci$_{155}$. LppRNAi discs accumulated ectopically stabilized Ci$_{155}$ in the nucleus within 1.5 hours after drug addition – a time frame that is consistent with that required for Ci$_{155}$ nuclear accumulation near the AP boundary in wild-type discs (Fig. 1O,P; see also Fig. S2C,D in the supplementary material). Thus, increased levels of basolateral Smo in LppRNAi discs cause Ci$_{155}$ stabilization and allow more Ci$_{155}$ to enter the nucleus, but are insufficient for target gene activation (Fig. 1Q,R) (Panáková et al., 2005). These data suggest that Ci$_{155}$ stabilization may be controlled by the amount of basolateral Smo, but that other signals are required for Smo to enable Ci$_{155}$ to act as a transcription factor. Lpp is required for normal Smo trafficking, but does not regulate Smo-dependent target gene activation.

The lipid contents of Lpp reduce basolateral Smo accumulation and reduce levels of Ci$_{155}$

To distinguish whether intact Lpp particles were required to reduce Smo and Ci$_{155}$ stability, or whether their lipid contents alone might suffice, we extracted lipids from purified Lpp particles, dried them and resuspended them into protein-free liposomes. The apolipophorin protein moiety is undetectable in these liposomes (see Fig. S2G in the supplementary material). We then incubated discs from LppRNAi animals with liposomes containing Lpp-derived lipids for 2 hours at a concentration that approximated that of the hemolymph. This treatment reverses the basolateral accumulation of Smo in LppRNAi discs to wild-type levels (Fig. 2A-E). Lpp lipids also reversed Ci$_{155}$ accumulation in a subset (*n*=27/54) of discs (see Fig. S2H-K in the supplementary material). Incubation with Lpp-derived lipids does not generally decrease levels of basolateral proteins since Arrow accumulation is unaffected in these discs (see Fig. S2L-O in the supplementary material) and similar treatment with medium alone had no effect on Smo (Fig. 2A,C); neither did liposomes containing two of the most abundant Lpp lipids, phosphatidylcholine and ergosterol (see Fig. S2P-S and Fig. S8A in the supplementary material). Thus, although Lpp lipids do not generally affect the trafficking of basolateral membrane proteins, they specifically reduce levels of basolateral Smo and consequently destabilize Ci$_{155}$.

The Ptc SSD makes Lpp-derived lipids available for Smo repression

How do Lpp lipids decrease Smo levels? One possibility is that they regulate the levels or activity of Ptc. If so, addition of these lipids to Ptc mutant cells would not be expected to reverse ectopic Smo accumulation. Alternatively, Ptc might mobilize lipids from Lpp particles, making them 'available' to destabilize Smo. In this case, the direct addition of lipids that have already been extracted from Lpp particles might reverse basolateral Smo accumulation in Ptc mutant cells. Lpp lipids did not reduce Smo accumulation in mutant clones that were totally missing the Ptc protein (Fig. 3A-D,I). However, interestingly, Lpp lipids did reduce Smo accumulation in tissue homozygous for *ptc^{S2}*, which harbors a point mutation in the SSD (Fig. 3E-H,J). This suggests that one function of the Ptc SSD is to make lipids within Lpp particles
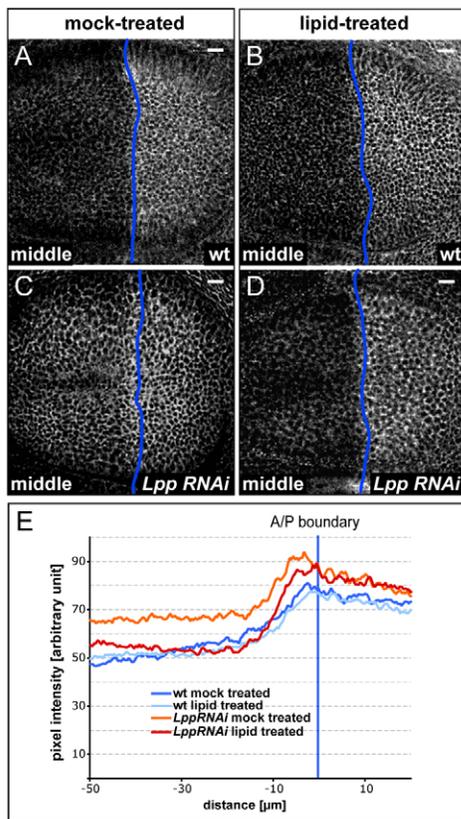
Fig. 2. Lpp-derived lipids reduce basolateral Smo accumulation.
(**A-D**) Smo staining in the middle region of a wild-type (A,B) or a
LppRNAi (C,D) wing disc treated (B,D) or not treated (A,C) with Lpp-
derived lipids. Ectopical Smo accumulation is reversed by treatment
with Lpp-derived lipids. (**E**) Quantification of Smo staining of wild-type
and LppRNAi discs either treated or not treated with Lpp lipids. At least
six discs were quantified for each condition. Lpp lipids rescue anterior
($P<0.0007$) but not posterior ($P<0.9032$) Smo accumulation in LppRNAi
discs. Lpp lipids do not elevate Smo staining intensity in either
compartment in wild-type discs ($P<0.4869$, $P<0.3175$). AP boundaries
are indicated by blue lines. Scale bars: 10 μm.

available to regulate Smo trafficking. However, it is clear that the
Lpp lipids are insufficient to destabilize Smo when the Ptc protein
is totally absent. Regulation of Smo trafficking by Ptc requires not
only a functional SSD, but also an intact C-terminal tail (Lu et al.,
2006). Thus, Lpp lipids may need to act in conjunction with the
Ptc C terminus to destabilize Smo.

Ptc diverts a subset of internalized Lpp to Ptc-positive endosomes

How might Ptc regulate the access of Lpp lipids to Smo? NPC1
promotes the exit of LDL-derived cholesterol and many other lipids
from late endosomes (Ikonen and Holtta-Vuori, 2004; Mukherjee
and Maxfield, 2004; Wojtanik and Liscum, 2003). Might Ptc act
similarly? When overexpressed, Ptc causes Lpp accumulation and
colocalizes with it in early endosomes (Fig. 4A-C; see also Fig.
S3K-M in the supplementary material) (Callejo et al., 2008). Ptc
overexpression does not obviously alter the size or number of either
Rab5- or Rab7-positive endosomes, suggesting that it does not
generally retard progression from early to late endosomes (see Fig.
S3A-D in the supplementary material) (Rink et al., 2005).

Furthermore, Lpp does not accumulate in cells overexpressing
NPC1 (see Fig. S3E,F in the supplementary material). Thus, Ptc
specifically recruits Lpp particles to Ptc-positive endosomes.

To investigate which regions of Ptc were required to cause Lpp
accumulation, we overexpressed different mutant forms of Ptc in the
dorsal compartment (for expression levels, see Fig. S3G in the
supplementary material). We found that removal of the Ptc C-
terminal tail, which is required for Smo repression, prevented Ptc-
mediated Lpp accumulation (Fig. 4D,E). The C-terminal tail is also
required for Ptc internalization and turnover (Lu et al., 2006).
Another internalization-defective Ptc allele, Ptc^{14}, also fails to cause
Lpp accumulation when overexpressed (Callejo et al., 2008),
suggesting that Ptc must be internalized to cause Lpp accumulation
in endosomes. Although the SSD is required for Smo repression, it
is not required for the accumulation of Lpp in endosomes with Ptc
(Fig. 4F,G), consistent with results from Callejo et al. (Callejo et al.,
2008). Thus, although Ptc SSD mutants can recruit Lpp to Ptc-
positive endosomes, they cannot make use of their contents to
destabilize Smo. Finally, a Ptc mutant missing sequences that are
required for binding to Hh nevertheless efficiently recruits Lpp to
Ptc endosomes (Fig. 4H,I). Consistent with this, expression of wild-
type Ptc causes Lpp accumulation even in a hh^{ts} mutant background
(see Fig. S3H-J in the supplementary material). Thus, although Hh
is present on some Lpp particles, Ptc affects Lpp trafficking
independently of Hh.

To distinguish whether the Lpp accumulation caused by Ptc
resulted from increased Lpp uptake or decreased Lpp degradation,
we performed uptake experiments with Alexa 546-labeled Lpp
particles. Discs overexpressing Ptc in the dorsal compartment were
incubated for 10 minutes at 22°C with labeled Lpp, then washed,
fixed and stained. After the 10-minute incubation, labeled Lpp
particles are present in endosomes throughout the wing disc and are
equally abundant in the dorsal and ventral compartments (Fig. 4J-
L). In the dorsal compartment, the vast majority of Lpp-Alexa 546
colocalizes with overexpressed Ptc in Rab5-positive endosomes (see
Fig. S4A-F in the supplementary material). Thus, although Ptc and
Lpp-Alexa 546 are incorporated rapidly into the same endosomes,
Ptc overexpression does not increase the rate of Lpp-Alexa 546
uptake. By contrast, overexpression of the LDL receptor homologue
LpR1-GFP does increase the rate of Lpp uptake, as expected (see
Fig. S4G-J in the supplementary material), indicating that this assay
is sensitive to such changes. After washing and incubation for a
further 20-40 minutes in Lpp-free medium, Lpp particles begin to
disappear from ventral compartment cells but are visible for up to
20 minutes in Ptc-overexpressing cells (Fig. 4M-O). By 40 minutes,
Lpp is mostly degraded in both compartments (see Fig. S4K,L in the
supplementary material). These data show that Ptc decreases the rate
of Lpp degradation after internalization, but does not increase Lpp
uptake. Thus, Ptc is unlikely to be an endocytic receptor for Lpp.

Since Ptc did not appear to promote Lpp uptake, we wondered
whether any of the canonical lipoprotein receptors might be required
for normal Hh signaling. We tested requirements for Megalin, the
LDL receptor protein LRP1, Arrow, and the two LDL receptor
homologues LpR1 and LpR2, using both mutagenesis and RNAi-
mediated knockdown. None of these mutants altered Lpp
accumulation in the steady state or produced Hh phenotypes similar
to those caused by LppRNAi (see Figs S5-S7 in the supplementary
material). These data indicate that multiple redundant mechanisms
may contribute to lipoprotein uptake in the wing disc, and that none
of these LDL receptor family proteins is individually required for
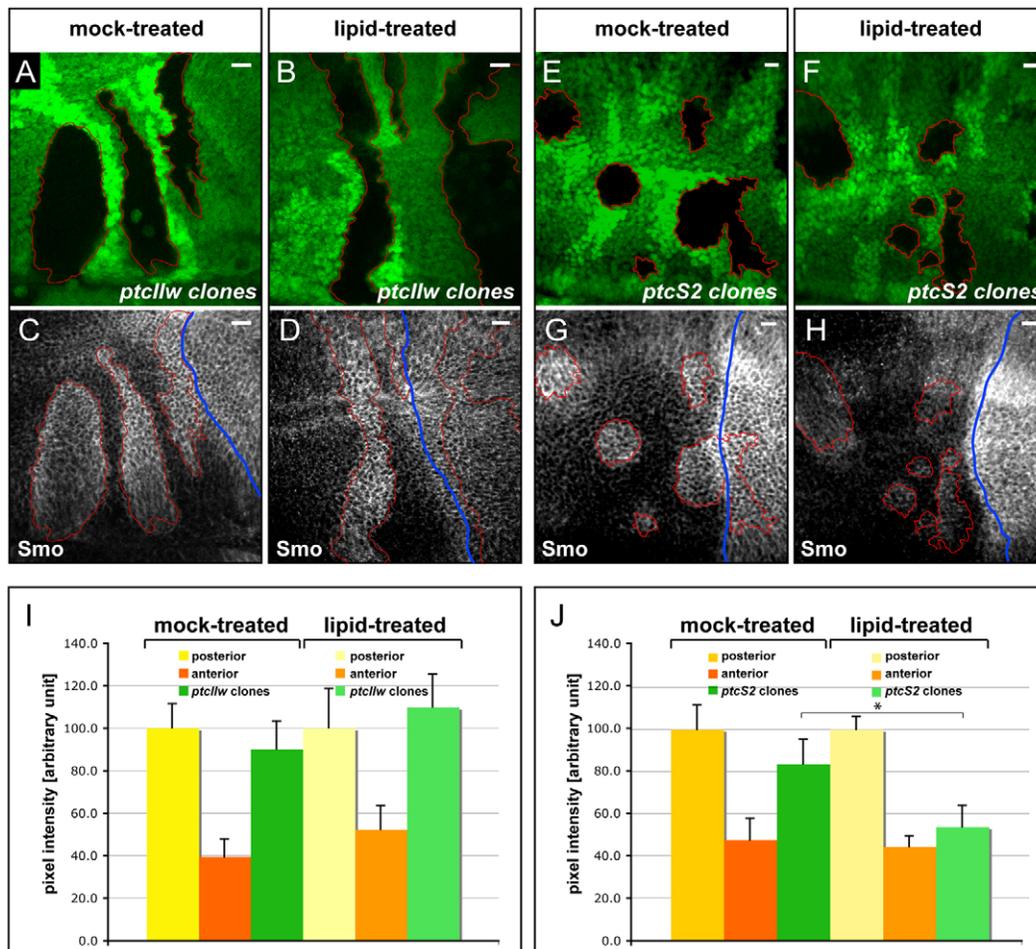the Lpp trafficking pathways that are relevant to Ptc-mediated Smo
repression.

Fig. 3. Lpp acts with Ptc to influence Smo trafficking. (**A-H**) Basolateral region of wing discs harboring either *ptc^llw* (A-D) or *ptc^S2* (E-H) mutant clones, indicated by the loss of GFP in A, B, E and F, either treated with Lpp lipids (B,D,F,H) or mock treated (A,C,E,G), then stained for Smo (C,D,G,H). *ptc^llw* is an amorphic allele harboring a nonsense mutation at codon 43. *ptc^S2* is a missense mutation substituting Asn for Asp at position 583 in the SSD (the identical mutation contained in the *Ptc^SSD* transgene). *ptc^S2* also contains a silent Val to Met substitution at position 1392 (Martin et al., 2001). (**I,J**) Quantification of Smo staining intensity in discs harboring *ptc^llw* (I) or *ptc^S2* (J) clones either treated or not treated with Lpp lipids. At least six clones were quantified for each condition. Yellow bars: staining intensity in the posterior compartment. Red bars: staining intensity in the anterior compartment (not the AP boundary). Green bars: staining intensity in the clones. Smo staining intensity is not significantly reduced by Lpp lipids in *ptc^llw* clones, but is reduced in *ptc^S2* clones ($P=1.6\times10^{-13}$). AP boundaries are indicated by blue lines. Scale bars: 10 µm.

Although Ptc can elevate Lpp levels when overexpressed, the endogenous Ptc present in the anterior compartment is not sufficient to obviously increase Lpp accumulation there (note the Lpp levels in the wild-type ventral compartment in Fig. 4A,B). This suggests that Ptc influences the trafficking of only a small fraction of Lpp when expressed at endogenous levels. This is not surprising, considering its important nutritional functions and the large number of different receptors with the potential to contribute to Lpp trafficking in the wing disc (see Fig. S5A-D in the supplementary material). In order to detect the effect of Ptc on Lpp in the anterior compartment in wild-type discs, we exploited the fact that Lpp in these endosomes should be degraded more slowly than most of the Lpp internalized by disc cells. To specifically visualize Lpp that was degraded more slowly than average, we placed dissected discs in Grace's medium for 2 hours. In this time, most Lpp that was internalized in vivo should pass through the degradative pathway and disappear, revealing the tissue distribution of any Lpp subpopulation with a longer half-life. Immunostaining discs after a 2-hour incubation in Grace's medium reveals a stable population of

Lpp that is found specifically in the anterior compartment, where Ptc is expressed (Fig. 4P-R). These data support the idea that, whereas most Lpp is internalized and degraded rapidly, Ptc redirects trafficking of a small subset of Lpp particles to a more stable endocytic compartment. Sequestration of Lpp by Ptc in these endosomes might give Ptc access to Lpp-derived lipids. We note that Lpp stability is increased uniformly throughout the anterior compartment and is not further increased near the AP boundary where Ptc is upregulated (but repressed by Hh). This may suggest that Hh interferes with Ptc-dependent Lpp trafficking.

Mutation of the Ptc SSD perturbs lipid trafficking from Ptc endosomes

The SSD of NPC1 is required for efflux of sterols, sphingolipids and other lipids from late endosomes. These include lipids derived from internalized lipoprotein particles (Ikonen and Holtta-Vuori, 2004; Mukherjee and Maxfield, 2004; Wojtanik and Liscum, 2003). Flies do not synthesize sterols (Clayton, 1964) and rely on Lpp for sterol delivery to discs (see Fig. S1A,C; Fig. S8A in the supplementary
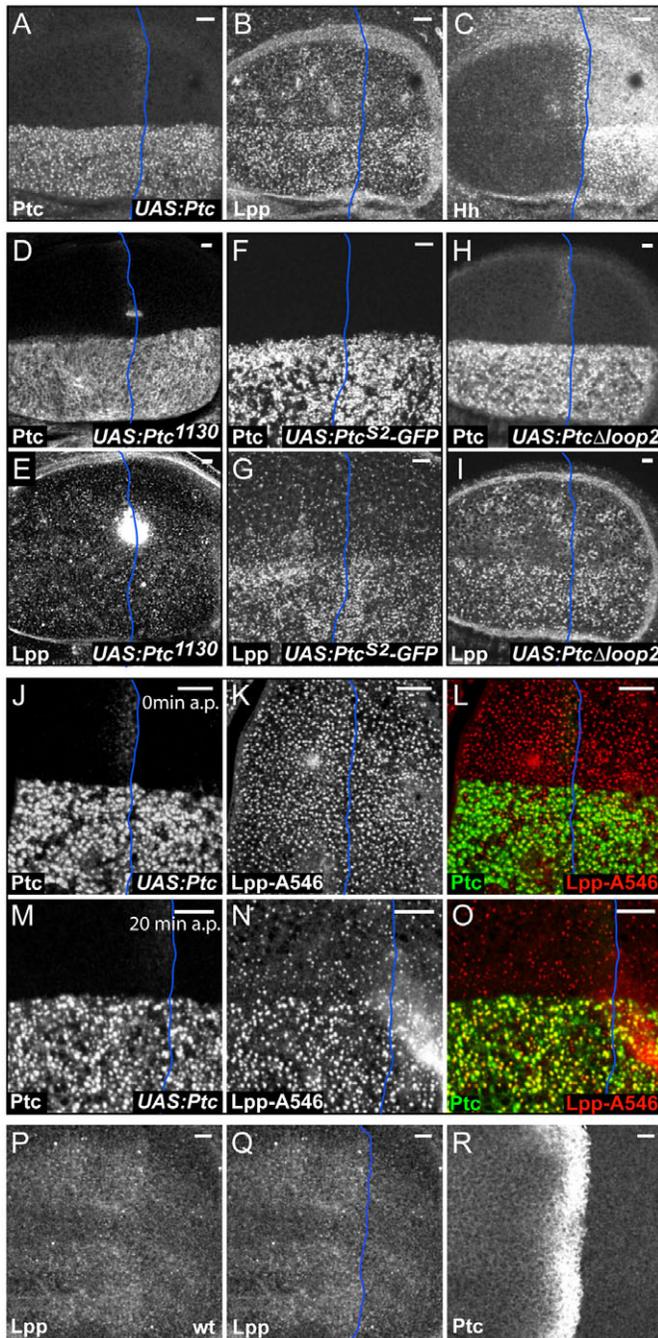
Fig. 4. Ptc does not increase Lpp uptake but increases its stability after internalization. All images show confocal sections in the apical region. (**A-C**) A wing disc overexpressing Ptc in the dorsal compartment for 18 hours, stained for Ptc (A), Lpp (B) and Hh (C). Ptc overexpression causes Lpp accumulation. The ratio of average staining intensity in the dorsal and ventral (Lpp_D:Lpp_V) compartments is 1.5:1. (**D,E**) A wing disc overexpressing the mutant Ptc^{1130}, which is not well internalized (Lu et al., 2006), in the dorsal compartment for 18 hours, stained for Ptc (D) and Lpp (E). Ptc^{1130} does not cause Lpp accumulation (Lpp_D:Lpp_V=1:1). (**F,G**) A wing disc overexpressing the mutant Ptc^{S2}-GFP in the dorsal compartment for 18 hours, stained for Ptc (F) and Lpp (G). Mutating the SSD does not prevent Lpp accumulation (Lpp_D:Lpp_V=1.6:1). (**H,I**) A wing disc overexpressing the mutant $Ptc^{\Delta loop2}$ in the dorsal compartment for 18 hours, stained for Ptc (H) and Lpp (I). Although it cannot bind to Hh, $Ptc^{\Delta loop2}$ recruits Lpp (Lpp_D:Lpp_V=1.4:1). (**J-L**) Internalization of purified and fluorescently labeled Lpp (Lpp-Alexa 546) by a wing disc overexpressing Ptc in the dorsal compartment. The disc was incubated for 10 minutes with Lpp-Alexa 546, then washed and fixed immediately (0 minutes after pulse=0 a.p.). Ptc (J,L, green) and Lpp (K,L, red) colocalize within 10 minutes (64.9% of Ptc colocalizes with Lpp, 73.0% of Lpp colocalizes with Ptc; *P* value$_{Costes}$=1.0). Lpp internalization does not increase in Ptc-overexpressing cells. (**M-O**) A wing disc overexpressing Ptc (M,O, green) after a 10-minute incubation with Lpp-Alexa 546, wash and a further 20-minute incubation in medium alone (20 minutes after pulse=20 a.p.). Lpp-positive endosomes are still abundant in Ptc-overexpressing tissue, whereas they are degraded much faster in wild-type tissue (N,O, red). Thus, Ptc slows Lpp degradation (Lpp_D:Lpp_V=1.5:1). (**P-R**) Wild-type wing disc incubated in Grace's medium for 2 hours and stained for Lpp (P,Q) and Ptc (R). The ratio of average staining intensity in the posterior and anterior (Lpp_P:Lpp_A) compartments is 1.2:1. Lpp is retained preferentially in the anterior compartment cells where Ptc is expressed. AP boundaries are indicated by blue lines. Scale bars: 10 μm.

specificities (Piddock, 2006) and many non-sterol lipids accumulate in NPC1 mutant endosomes, it is possible that Ptc SSD activity also regulates the accumulation of other lipids.

Although it seems likely that the accumulated sterol in Ptc^{SSD}-positive endosomes is derived from sequestered Lpp, it is also possible that membrane sterol, previously delivered by Lpp, is also trapped by mutation of the Ptc SSD. To confirm that sterols that have been newly delivered by Lpp contribute to endosomal sterol accumulation, we fed larvae with BODIPY-cholesterol (Holtta-Vuori et al., 2008) coincident with induction of Ptc or Ptc^{SSD} overexpression. BODIPY-cholesterol accumulates in cells overexpressing Ptc^{SSD} but not wild-type Ptc (see Fig. S8B-G in the supplementary material). Thus, at least part of the accumulated sterol has been delivered to discs subsequent to the induction of Ptc expression.

Because endogenous Ptc normally sequesters only a small subset of internalized Lpp, it is unlikely to be required for endosomal sterol efflux in general – indeed, sterol does not accumulate abnormally in ptc^{S2} mutant clones (not shown). However, these data indicate that endogenous Ptc probably influences the membrane lipid composition of the subset of endosomes in which it is present. How could the lipid composition of Ptc endosomes affect Smo? A clue emerged when we compared the distribution of Smo in cells overexpressing wild-type Ptc with cells overexpressing Ptc^{SSD}. Wild-type Ptc overexpression inactivates Smo signaling and reduces Smo levels on the basolateral membrane in both anterior and posterior compartments (Martin et al., 2001) (see Fig. S8I in the supplementary material). No Smo is detectable in apical endosomes (see Fig. S8H in the supplementary material). By striking contrast,
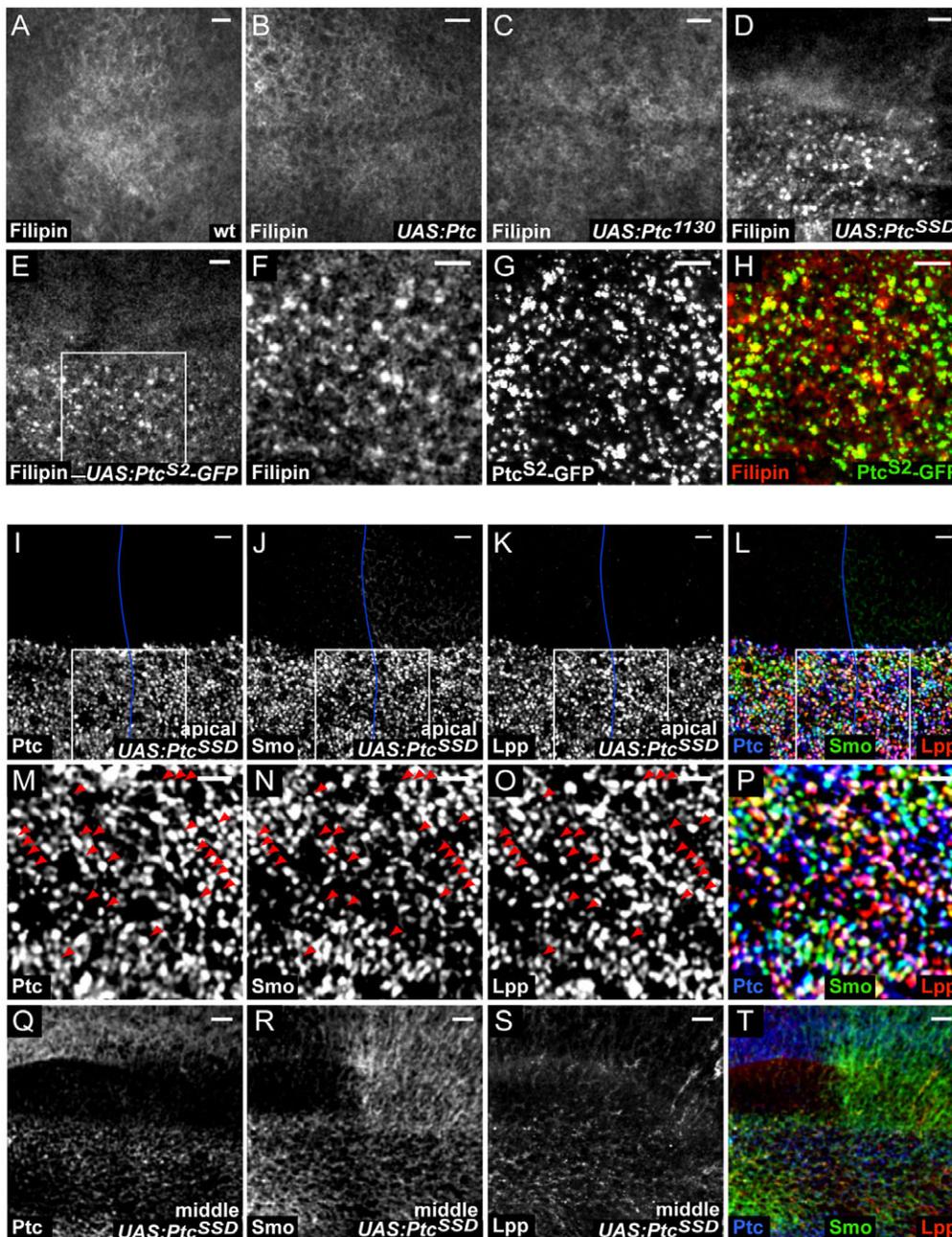
material). To test whether the Ptc SSD influenced the trafficking of Lpp lipids from Ptc-positive endosomes, we examined sterol distribution in cells overexpressing wild-type and mutant forms of Ptc (for expression levels, see Fig. S3G in the supplementary material). Although wild-type Ptc sequesters Lpp in endosomes, filipin staining shows that it does not perturb sterol distribution (Fig. 5A,B). By contrast, both Ptc^{S2} and Ptc^{SSD}, which also sequester Lpp, cause sterol accumulation in Ptc positive endosomes (Fig. 5D-H). Thus, the SSD is required for the exit of sterols from this compartment. Ptc^{1130} overexpression does not cause endosomal sterol accumulation (Fig. 5C) – consistent with its inability to sequester Lpp in endosomes. These data suggest that Ptc sequesters Lpp particles in endosomes and mobilizes their lipid contents via its SSD. Since RND transporters have extremely broad substrate

Fig. 5. Mutation of the Ptc SSD prevents endosomal sterol efflux and traps Smo in Ptc endosomes. (**A**) Subapical region of a wild-type wing disc stained with filipin. (**B-H**) Subapical region of discs expressing the following different Ptc variants in the dorsal compartment: wild-type Ptc (B), Ptc[1130] (C), Ptc[SSD] (D), Ptc[S2]-GFP (E-H). (F-H) Magnified images of the region boxed in E: filipin staining (F,H, red) and Ptc[S2]-GFP (G,H, green). Ptc[SSD] and Ptc[S2]-GFP cause sterol accumulation in Ptc endosomes, whereas wild-type Ptc and Ptc[1130] do not (68.7% of Ptc[S2]-GFP colocalizes with filipin, 88.9% of filipin colocalizes with Ptc[S2]-GFP; P value$_{Costes}$=1.0). (**I-P**) Apical section of a wing disc, which has been overexpressing Ptc[SSD] in the dorsal compartment for 18 hours, stained for Ptc (I,L,M,P, blue), Smo (J,L,N,P, green) and Lpp (K,L,O,P, red). (M-P) Magnified images of the region boxed in I-L. Ptc[SSD] overexpression causes accumulation of Smo in Ptc- and Lpp-positive apical endosomes. Red arrowheads indicate examples of triple colocalization. In the dorsal compartment, 94.4% of Ptc colocalizes with Lpp, 94.8% of Ptc colocalizes with Smo, 91.6% of Lpp colocalizes with Ptc, 96.7% of Lpp colocalizes with Smo, 81.8% of Smo colocalizes with Ptc, 85.9% of Smo colocalizes with Lpp; P value$_{Costes}$=1.0. (**Q-T**) Basolateral region of a wing disc overexpressing Ptc[SSD] in the dorsal compartment for 18 hours, stained for Ptc (Q,T, blue), Smo (R,T, green) and Lpp (S,T, red). Overexpression of Ptc[SSD] elevates basolateral Smo. AP boundaries are indicated by blue lines. Scale bars: 10 μm.

Ptc[SSD] expression causes a dramatic accumulation of Smo in apical endosomes together with Ptc[SSD] and Lpp (Fig. 5I-P). In the anterior compartment, Ptc[SSD] expression also elevates basolateral Smo levels (Fig. 5Q-T), consistent with activation of Smo signaling in these cells (see Fig. S8R,S in the supplementary material). This suggests that Ptc[SSD] mutations specifically block Smo trafficking towards degradation – perhaps indirectly increasing Smo recycling (see Marois et al., 2006). To ask whether Ptc[SSD] overexpression might generally perturb the trafficking of basolateral membrane proteins, we examined the localization of FasIII and Arrow (see Fig. S8J-O in the supplementary material). Unlike Smo, neither FasIII nor Arrow accumulates in endosomes with Ptc[SSD], nor are their levels on the basolateral membrane altered. Thus, mutation of the Ptc SSD specifically affects trafficking of both Lpp lipids and Smo without perturbing localization of other basolateral membrane proteins.

To ask whether mutation of the Ptc SSD caused endosomal Smo accumulation when expressed at endogenous levels, we examined Smo localization in *ptc[S2]* mutant cells. Similar, although less dramatic, colocalization of Ptc[S2], Smo and Lpp in punctate structures is also observed in *ptc[S2]* mutant tissue (Fig. 6A-I), consistent with the idea that the Ptc SSD is required for normal endosomal trafficking of Smo. Taken together, these observations indicate that Smo may normally traffic through Ptc endosomes, and that blocking Ptc SSD activity not only causes endosomal lipid accumulation but also alters the trafficking of Smo from this compartment.

DISCUSSION
A central feature of the Hh pathway is repression of Smo signaling by Ptc when Hh is absent. How this repression functions at a mechanistic level is not understood. Ptc represses Smo at
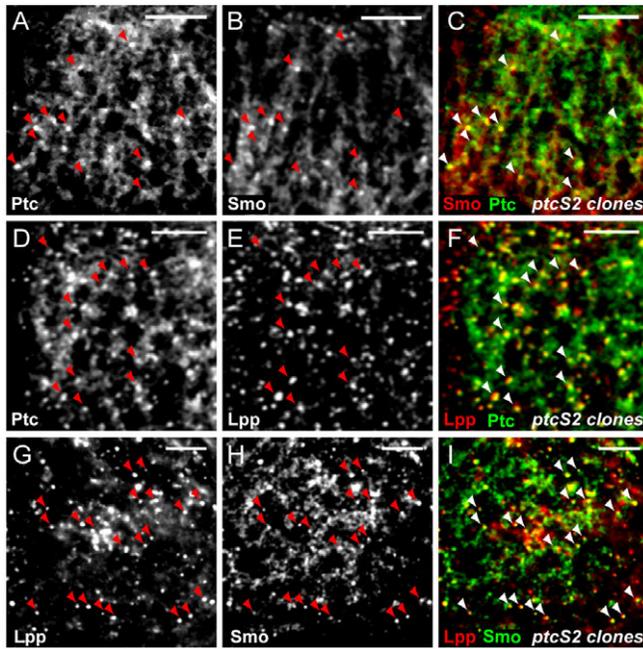
Fig. 6. Effects of SSD mutation on Smo trafficking. All images show apical confocal sections. (**A-C**) A *ptc^S2* clone stained for Ptc (A,C, green) and Smo (B,C, red). (**D-F**) A *ptc^S2* clone stained for Ptc (D,F, green) and Lpp (E,F, red). (**G-I**) A *ptc^S2* clone stained for Lpp (G,I, red) and Smo (H,I, green). Smo is found in punctate structures containing Ptc^S2 and Lpp. Examples of colocalization are indicated by arrowheads (C,F,I). AP boundaries are indicated by blue lines. Scale bars: 10 μm.

correlates with changes in Smo subcellular localization and decreased stability (Denef et al., 2000).

Models for Ptc-mediated repression have been proposed based on its SSD and on its sequence similarity to RND family transporters. Membrane sterol levels can alter trafficking and/or the stability of other proteins with SSDs (Kuwabara and Labouesse, 2002), thus it has been proposed that lipids might control the repressive activity of Ptc. Alternatively, based on its similarity to RND transporters, it has been proposed that Ptc might regulate Smo by modulating lipid trafficking. This is an attractive idea because Smo activity can be regulated by small lipophilic molecules (Chen et al., 2002a; Chen et al., 2002b; Frank-Kamenetsky et al., 2002). Although these are plausible models, there has as yet been no evidence to suggest that Ptc alters lipid trafficking or that any lipid alters Ptc function. Furthermore, if Ptc did regulate lipid transport to repress Smo, it is not clear where contact between Smo and Ptc-mobilized lipids would occur.

We now show that one or more lipids derived from the *Drosophila* lipoprotein Lpp are required for normal Ptc-mediated Smo destabilization. Ptc sequesters a small fraction of internalized Lpp in the Ptc-positive endosomal compartment and regulates lipid trafficking from this compartment via its SSD. Mutation of the Ptc SSD causes at least one Lpp-derived lipid, sterol, to accumulate in Ptc endosomes. Given that RND permeases have rather broad substrate specificities (Piddock, 2006), Ptc SSD mutation may also perturb the trafficking of additional lipids from this compartment. Similar mutations in NPC1 alter endosomal trafficking of sphingolipids, as well as sterols (Ikonen and Holtta-Vuori, 2004; Mukherjee and Maxfield, 2004; Wojtanik and Liscum, 2003).

Although Ptc-dependent sterol trafficking is clearly dependent on its SSD, Ptc has been reported to reduce the accumulation of neutral lipid in a manner that does not depend on its SSD. Rather, this effect of Ptc appears to depend on its ability to sequester Lpp (Callejo et
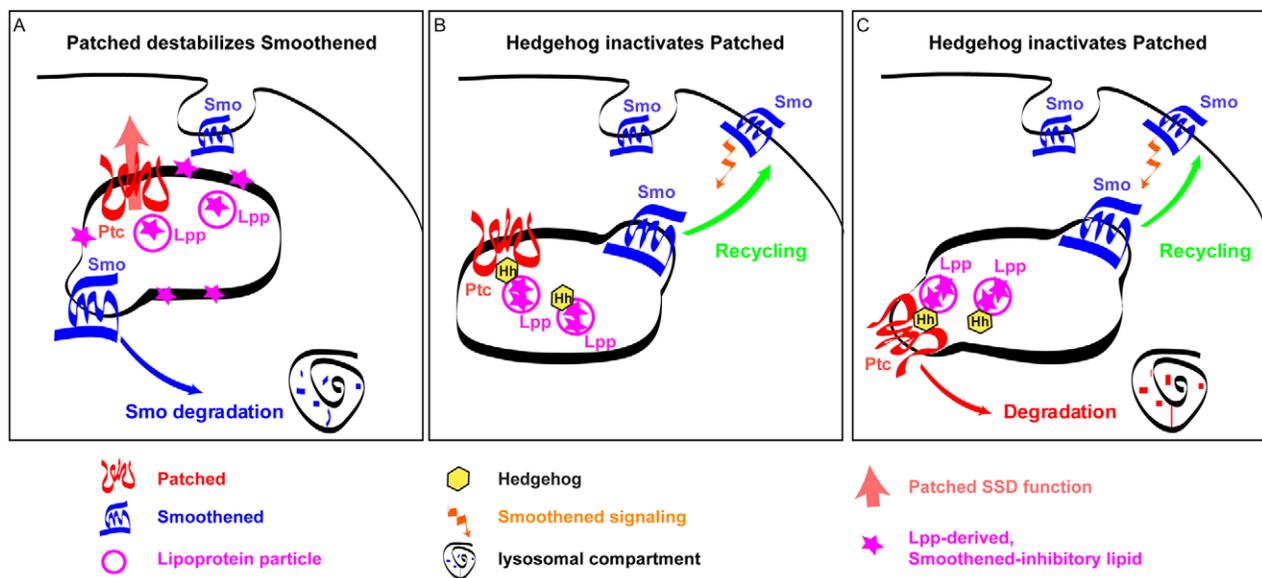
substoichiometric levels (Taipale et al., 2002) and the two proteins do not appear to be enriched at similar subcellular locations in the steady state in vivo (Martin et al., 2001). Repression of Smo by Ptc

Fig. 7. A model for Ptc control of Smo trafficking. Smo (blue) is internalized and moves through endosomes that contain Ptc (red) and Lpp (pink). From these endosomes, Smo is either sorted to degradation or recycled to the basolateral membrane. This decision is controlled by Ptc. Ptc regulates the lipid composition of these endosomes via its SSD – partly by promoting the mobilization of lipids derived from Lpp (pink stars). (**A**) Ptc destabilizes Smo. Here, Lpp lipids bias Smo trafficking towards degradation. (**B**) Hh blocks lipid mobilization by Ptc. Here, Hh (yellow) on Lpp particles inhibits the mobilization of inhibitory lipids by Ptc. This elevates Smo levels on the basolateral membrane. (**C**) Hh increases Ptc degradation. Here, Hh induces rapid degradation of Ptc and Lpp, thereby preventing Lpp sequestration and lipid mobilization. This elevates Smo levels on the basolateral membrane.

al., 2008). This may suggest that Ptc-mediated sequestration of Lpp diverts these particles away from trafficking pathways that promote neutral lipid storage.

Ptc is normally present in a small fraction of endosomes and, unlike NPC1, does not generally perturb cellular sterol trafficking when mutated. How could altered trafficking in the small subset of endosomes that contain Ptc affect Smo? We show that mutation of the Ptc SSD not only alters lipid trafficking in Ptc endosomes, but also causes Smo to accumulate in this compartment (as well as on the basolateral membrane). Similar endosomal colocalization between Ptc and Smo has been observed in vertebrate tissue culture cells (Incardona et al., 2002). This suggests that Smo normally traffics through Ptc endosomes, where it can be exposed to lipids that are mobilized by the Ptc SSD. Thus, Ptc may control the level of basolateral Smo by changing the balance of Smo degradation and recycling from Ptc endosomes. Lipid accumulation in endosomes of NPC1 mutant cells influences the activity of Rab7 (Lebrand et al., 2002), Rab9 (Ganley and Pfeffer, 2006) and Rab4 (Choudhury et al., 2004), perturbing degradation and recycling. The lipid composition of Ptc-positive endosomes may exert similar, but much more specific, effects on Smo, altering the total levels of Smo protein.

Which Lpp lipids does Ptc use to regulate Smo trafficking? Although sterols are present in Lpp and the Ptc SSD does regulate sterol trafficking from Ptc endosomes, our data do not support a role for bulk membrane sterol in Smo regulation. Membrane sterol can be reduced sixfold by dietary depletion without changing Smo levels on the basolateral membrane or other aspects of Hh signaling. Furthermore, liposome-mediated addition of ergosterol, the most abundant membrane sterol in *Drosophila* (Rietveld et al., 1999), does not reverse Smo accumulation caused by LppRNAi. However, our data do not rule out the possibility that signaling sterol derivatives that act at low concentrations might be responsible. We are now fractionating Lpp lipid extracts to identify this active molecule.

Loss of Lpp reproduces only a subset of the effects of Ptc mutation on Smo signaling – although it stabilizes Smo and causes Smo-dependent accumulation of full-length Ci_{155}, it does not allow target gene activation. Similar uncoupling of Ci_{155} stability and target gene activation is seen in *fused* and *dally* mutants (Alves et al., 1998; Eugster et al., 2007; Wang and Holmgren, 1999). It seems unlikely that 'activation' of Ci_{155} simply requires higher levels of Smo than Ci_{155} stabilization; in LppRNAi discs, Smo levels reach those that result in target gene activation in wild-type discs over a broader region than in wild-type discs – nevertheless, the range of target gene activation is narrowed. Rather, these data suggest that, although Ci_{155} stabilization is regulated by the level of Smo on the basolateral membrane, its activation as a transcription factor requires a separate Smo-dependent signal. Similarly, in vertebrate cells, where Ptc regulates Smo trafficking to the primary cilium, it is clear that ciliary localization is insufficient for Smo signaling to activate transcription of target genes (Aanstad et al., 2009; Rohatgi et al., 2009; Wang et al., 2009). Other G-protein-coupled receptors activate multiple signal transduction pathways in response to different ligands (Perez and Karnik, 2005). Thus, Smo trafficking and Smo activation may also be controlled by different ligands. Although Lpp lipids regulate Smo trafficking, other lipids mobilized by Ptc could have additional effects on Smo signaling activity.

A model for Ptc-mediated Smo destabilization

The following model (Fig. 7) would be consistent with what is already known of Ptc-dependent Smo regulation and with our new observations. Ptc sequesters Lpp into Ptc-positive endosomes and

regulates lipid trafficking in this compartment via its SSD. Smo that passes through Ptc endosomes can be targeted either for degradation or recycling, depending on Ptc-dependent modulation of endosomal lipid composition, and on other functions of the Ptc protein. Lipids derived from Lpp particles bias Smo trafficking towards degradation (Fig. 7A). The balance of degradation versus recycling affects total Smo levels on the basolateral membrane and its ability to stabilize Ci_{155}.

The association of Hh with Lpp may do more than simply promote the release of Hh from the membrane. Hh is thought to bind to the extracellular loops of Ptc (Marigo et al., 1996) – a region that is important for conferring substrate specificity in RND family transporters (Elkins and Nikaido, 2002; Mao et al., 2002). The presence of Hh on lipoproteins may block Ptc-mediated mobilization of their lipids (Fig. 7B). Alternatively, increased Ptc degradation upon Hh binding may prevent Lpp sequestration and lipid mobilization (Fig. 7C). In either case, association with Lpp particles efficiently positions Hh to interfere with, or alter, the mobilization of Lpp lipid contents by Ptc, helping to alleviate Ptc-mediated Smo repression. Thus, Hh may signal, in part, by influencing the utilization of the lipoprotein particles on which it is carried.

References

Aanstad, P., Santos, N., Corbit, K. C., Scherz, P. J., le Trinh, A., Salvenmoser, W., Huisken, J., Reiter, J. F. and Stainier, D. Y. (2009). The extracellular domain of Smoothened regulates ciliary localization and is required for high-level Hh signaling. *Curr. Biol.* **19**, 1034-1039.

Alves, T. L., Costa, A. C., Henriques, A. W. and Lima, E. L. (1998). Adaptive optimal control of fed-batch alcoholic fermentation. *Appl. Biochem. Biotechnol.* **70-72**, 463-478.

Aza-Blanc, P. and Kornberg, T. B. (1999). Ci: a complex transducer of the hedgehog signal. *Trends Genet.* **15**, 458-462.

Aza-Blanc, P., Ramirez-Weber, F. A., Laget, M. P., Schwartz, C. and Kornberg, T. B. (1997). Proteolysis that is inhibited by hedgehog targets Cubitus interruptus protein to the nucleus and converts it to a repressor. *Cell* **89**, 1043-1053.

Blackman, R. K., Sanicola, M., Raftery, L. A., Gillevet, T. and Gelbart, W. M. (1991). An extensive 3′ cis-regulatory region directs the imaginal disk expression of decapentaplegic, a member of the TGF-beta family in Drosophila. *Development* **111**, 657-666.

Bligh, E. G. and Dyer, W. J. (1959). A rapid method of total lipid extraction and purification. *Can. J. Biochem. Physiol.* **37**, 911-917.

Briscoe, J., Chen, Y., Jessell, T. M. and Struhl, G. (2001). A hedgehog-insensitive form of patched provides evidence for direct long-range morphogen activity of sonic hedgehog in the neural tube. *Mol. Cell* **7**, 1279-1291.

Burke, R., Nellen, D., Bellotto, M., Hafen, E., Senti, K. A., Dickson, B. J. and Basler, K. (1999). Dispatched, a novel sterol-sensing domain protein dedicated to the release of cholesterol-modified hedgehog from signaling cells. *Cell* **99**, 803-815.

Callejo, A., Culi, J. and Guerrero, I. (2008). Patched, the receptor of Hedgehog, is a lipoprotein receptor. *Proc. Natl. Acad. Sci. USA* **105**, 912-917.

Chen, J. K., Taipale, J., Cooper, M. K. and Beachy, P. A. (2002a). Inhibition of Hedgehog signaling by direct binding of cyclopamine to Smoothened. *Genes Dev.* **16**, 2743-2748.

Chen, J. K., Taipale, J., Young, K. E., Maiti, T. and Beachy, P. A. (2002b). Small molecule modulation of Smoothened activity. *Proc. Natl. Acad. Sci. USA* **99**, 14071-14076.

Chen, Y. and Struhl, G. (1998). In vivo evidence that Patched and Smoothened constitute distinct binding and transducing components of a Hedgehog receptor complex. *Development* **125**, 4943-4948.

Choudhury, A., Sharma, D. K., Marks, D. L. and Pagano, R. E. (2004). Elevated endosomal cholesterol levels in Niemann-Pick cells inhibit rab4 and perturb membrane recycling. *Mol. Biol. Cell* **15**, 4500-4511.

Clayton, R. B. (1964). The Utilization Of Sterols By Insects. *J. Lipid Res.* **15**, 3-19.

Corbit, K. C., Aanstad, P., Singla, V., Norman, A. R., Stainier, D. Y. and Reiter, J. F. (2005). Vertebrate Smoothened functions at the primary cilium. *Nature* **437**, 1018-1021.

Corcoran, R. B. and Scott, M. P. (2006). Oxysterols stimulate Sonic hedgehog signal transduction and proliferation of medulloblastoma cells. *Proc. Natl. Acad. Sci. USA* **103**, 8408-8413.

Costes, S. V., Daelemans, D., Cho, E. H., Dobbin, Z., Pavlakis, G. and Lockett, S. (2004). Automatic and quantitative measurement of protein-protein colocalization in live cells. *Biophys. J.* **86**, 3993-4003.

Culi, J. and Mann, R. S. (2003). Boca, an endoplasmic reticulum protein required for wingless signaling and trafficking of LDL receptor family members in Drosophila. *Cell* **112**, 343-354.

Dellovade, T., Romer, J. T., Curran, T. and Rubin, L. L. (2006). The hedgehog pathway and neurological disorders. *Annu. Rev. Neurosci.* **29**, 539-563.

Denef, N., Neubuser, D., Perez, L. and Cohen, S. M. (2000). Hedgehog induces opposite changes in turnover and subcellular localization of patched and smoothened. *Cell* **102**, 521-531.

Dwyer, J. R., Sever, N., Carlson, M., Nelson, S. F., Beachy, P. A. and Parhami, F. (2007). Oxysterols are novel activators of the hedgehog signaling pathway in pluripotent mesenchymal cells. *J. Biol. Chem.* **12**, 8959-8968.

Elkins, C. A. and Nikaido, H. (2002). Substrate specificity of the RND-type multidrug efflux pumps AcrB and AcrD of Escherichia coli is determined predominantly by two large periplasmic loops. *J. Bacteriol.* **184**, 6490-6498.

Eugster, C., Panakova, D., Mahmoud, A. and Eaton, S. (2007). Lipoprotein-heparan sulfate interactions in the Hedgehog pathway. *Dev. Cell* **13**, 57-71.

Frank-Kamenetsky, M., Zhang, X. M., Bottega, S., Guicherit, O., Wichterle, H., Dudek, H., Bumcrot, D., Wang, F. Y., Jones, S., Shulok, J. et al. (2002). Small-molecule modulators of Hedgehog signaling: identification and characterization of Smoothened agonists and antagonists. *J. Biol.* **1**, 10.

Ganley, I. G. and Pfeffer, S. R. (2006). Cholesterol accumulation sequesters Rab9 and disrupts late endosome function in NPC1-deficient cells. *J. Biol. Chem.* **281**, 17890-17899.

Haycraft, C. J., Banizs, B., Aydin-Son, Y., Zhang, Q., Michaud, E. J. and Yoder, B. K. (2005). Gli2 and gli3 localize to cilia and require the intraflagellar transport protein polaris for processing and function. *PLoS Genet.* **1**, e53.

Holtta-Vuori, M., Uronen, R. L., Repakova, J., Salonen, E., Vattulainen, I., Panula, P., Li, Z., Bittman, R. and Ikonen, E. (2008). BODIPY-cholesterol: A new tool to visualize sterol trafficking in living cells and organisms. *Traffic* **11**, 1839-1849.

Huangfu, D. and Anderson, K. V. (2005). Cilia and Hedgehog responsiveness in the mouse. *Proc. Natl. Acad. Sci. USA* **102**, 11325-11330.

Huangfu, D. and Anderson, K. V. (2006). Signaling from Smo to Ci/Gli: conservation and divergence of Hedgehog pathways from Drosophila to vertebrates. *Development* **133**, 3-14.

Ikonen, E. and Holtta-Vuori, M. (2004). Cellular pathology of Niemann-Pick type C disease. *Semin. Cell Dev. Biol.* **15**, 445-454.

Incardona, J. P., Gruenberg, J. and Roelink, H. (2002). Sonic hedgehog induces the segregation of patched and smoothened in endosomes. *Curr. Biol.* **12**, 983-995.

Ingham, P. W. and Placzek, M. (2006). Orchestrating ontogenesis: variations on a theme by sonic hedgehog. *Nat. Rev. Genet.* **7**, 841-850.

Johnson, R. L., Milenkovic, L. and Scott, M. P. (2000). In vivo functions of the patched protein: requirement of the C terminus for target gene inactivation but not Hedgehog sequestration. *Mol. Cell* **6**, 467-478.

Kalderon, D. (2005). The mechanism of hedgehog signal transduction. *Biochem. Soc. Trans.* **33**, 1509-1512.

Kuwabara, P. E. and Labouesse, M. (2002). The sterol-sensing domain: multiple families, a unique role? *Trends Genet.* **18**, 193-201.

Lebrand, C., Corti, M., Goodson, H., Cosson, P., Cavalli, V., Mayran, N., Faure, J. and Gruenberg, J. (2002). Late endosome motility depends on lipids via the small GTPase Rab7. *EMBO J.* **21**, 1289-1300.

Lefers, M. A., Wang, Q. T. and Holmgren, R. A. (2001). Genetic dissection of the Drosophila Cubitus interruptus signaling complex. *Dev. Biol.* **236**, 411-420.

Lu, X., Liu, S. and Kornberg, T. B. (2006). The C-terminal tail of the Hedgehog receptor Patched regulates both localization and turnover. *Genes Dev.* **20**, 2539-2551.

Lum, L. and Beachy, P. A. (2004). The Hedgehog response network: sensors, switches, and routers. *Science* **304**, 1755-1759.

Lum, L., Zhang, C., Oh, S., Mann, R. K., von Kessler, D. P., Taipale, J., Weis-Garcia, F., Gong, R., Wang, B. and Beachy, P. A. (2003). Hedgehog signal

transduction via Smoothened association with a cytoplasmic complex scaffolded by the atypical kinesin, Costal-2. *Mol. Cell* **12**, 1261-1274.

Mao, W., Warren, M. S., Black, D. S., Satou, T., Murata, T., Nishino, T., Gotoh, N. and Lomovskaya, O. (2002). On the mechanism of substrate specificity by resistance nodulation division (RND)-type multidrug resistance pumps: the large periplasmic loops of MexD from Pseudomonas aeruginosa are involved in substrate recognition. *Mol. Microbiol.* **46**, 889-901.

Marigo, V., Davey, R. A., Zuo, Y., Cunningham, J. M. and Tabin, C. J. (1996). Biochemical evidence that patched is the Hedgehog receptor. *Nature* **384**, 176-179.

Marois, E., Mahmoud, A. and Eaton, S. (2006). The endocytic pathway and formation of the Wingless morphogen gradient. *Development* **133**, 307-317.

Marsh, J. B. and Weinstein, D. B. (1966). Simple charring method for determination of lipids. *J. Lipid Res.* **7**, 574-576.

Martin, V., Carrillo, G., Torroja, C. and Guerrero, I. (2001). The sterol-sensing domain of Patched protein seems to control Smoothened activity through Patched vesicular trafficking. *Curr. Biol.* **11**, 601-607.

McMahon, A. P., Ingham, P. W. and Tabin, C. J. (2003). Developmental roles and clinical significance of hedgehog signaling. *Curr. Top. Dev. Biol.* **53**, 1-114.

Mukherjee, S. and Maxfield, F. R. (2004). Lipid and cholesterol trafficking in NPC. *Biochim. Biophys. Acta* **1685**, 28-37.

Nybakken, K. and Perrimon, N. (2002). Hedgehog signal transduction: recent findings. *Curr. Opin. Genet. Dev.* **12**, 503-511.

Panáková, D., Sprong, H., Marois, E., Thiele, C. and Eaton, S. (2005). Lipoprotein particles are required for Hedgehog and Wingless signalling. *Nature* **435**, 58-65.

Pasca di Magliano, M. and Hebrok, M. (2003). Hedgehog signalling in cancer formation and maintenance. *Nat. Rev. Cancer* **3**, 903-911.

Perez, D. M. and Karnik, S. S. (2005). Multiple signaling states of G-protein-coupled receptors. *Pharmacol. Rev.* **57**, 147-161.

Piddock, L. J. (2006). Multidrug-resistance efflux pumps-not just for resistance. *Nat. Rev. Microbiol.* **4**, 629-636.

Riederer, M. A., Soldati, T., Shapiro, A. D., Lin, J. and Pfeffer, S. R. (1994). Lysosome biogenesis requires Rab9 function and receptor recycling from endosomes to the trans-Golgi network. *J. Cell Biol.* **125**, 573-582.

Rietveld, A., Neutz, S., Simons, K. and Eaton, S. (1999). Association of sterol- and glycosylphosphatidylinositol-linked proteins with Drosophila raft lipid microdomains. *J. Biol. Chem.* **274**, 12049-12054.

Rincon-Limas, D. E., Lu, C. H., Canal, I., Calleja, M., Rodriguez-Esteban, C., Izpisua-Belmonte, J. C. and Botas, J. (1999). Conservation of the expression and function of apterous orthologs in Drosophila and mammals. *Proc. Natl. Acad. Sci. USA* **96**, 2165-2170.

Rink, J., Ghigo, E., Kalaidzidis, Y. and Zerial, M. (2005). Rab conversion as a mechanism of progression from early to late endosomes. *Cell* **122**, 735-749.

Rohatgi, R., Milenkovic, L. and Scott, M. P. (2007). Patched1 regulates hedgehog signaling at the primary cilium. *Science* **317**, 372-376.

Rohatgi, R., Milenkovic, L., Corcoran, R. B. and Scott, M. P. (2009). Hedgehog signal transduction by Smoothened: pharmacologic evidence for a 2-step activation process. *Proc. Natl. Acad. Sci. USA* **106**, 3196-3201.

Ruiz i Altaba, A., Sanchez, P. and Dahmane, N. (2002). Gli and hedgehog in cancer: tumours, embryos and stem cells. *Nat. Rev. Cancer* **2**, 361-372.

Smelkinson, M. G., Zhou, Q. and Kalderon, D. (2007). Regulation of Ci-SCF(Slimb) Binding, Ci Proteolysis, and Hedgehog Pathway Activity by Ci Phosphorylation. *Dev. Cell* **13**, 481-495.

Strigini, M. and Cohen, S. M. (1997). A Hedgehog activity gradient contributes to AP axial patterning of the Drosophila wing. *Development* **124**, 4697-4705.

Strutt, H., Thomas, C., Nakano, Y., Stark, D., Neave, B., Taylor, A. M. and Ingham, P. W. (2001). Mutations in the sterol-sensing domain of Patched suggest a role for vesicular trafficking in Smoothened regulation. *Curr. Biol.* **11**, 608-613.

Taipale, J., Cooper, M. K., Maiti, T. and Beachy, P. A. (2002). Patched acts catalytically to suppress the activity of Smoothened. *Nature* **418**, 892-897.

Torroja, C., Gorfinkiel, N. and Guerrero, I. (2004). Patched controls the Hedgehog gradient by endocytosis in a dynamin-dependent manner, but this internalization does not play a major role in signal transduction. *Development* **131**, 2395-2408.

Tseng, T. T., Gratwick, K. S., Kollman, J., Park, D., Nies, D. H., Goffeau, A. and Saier, M. H., Jr (1999). The RND permease superfamily: an ancient, ubiquitous and diverse family that includes human disease and development proteins. *J. Mol. Microbiol. Biotechnol.* **1**, 107-125.

Wang, Q. T. and Holmgren, R. A. (1999). The subcellular localization and activity of Drosophila cubitus interruptus are regulated at multiple levels. *Development* **126**, 5097-5106.

Wang, Y., Zhou, Z., Walsh, C. T. and McMahon, A. P. (2009). Selective translocation of intracellular Smoothened to the primary cilium in response to Hedgehog pathway modulation. *Proc. Natl. Acad. Sci. USA* **106**, 2623-2628.

Wojtanik, K. M. and Liscum, L. (2003). The transport of low density lipoprotein-derived cholesterol to the plasma membrane is defective in NPC1 cells. *J. Biol. Chem.* **278**, 14850-14856.